

Sinter hardening material solutions for high performance applications

Dimitris Chasoglou¹, Ola Bergman¹

¹Höganäs AB, Höganäs, SE-26383, Sweden

*Corresponding author: dimitris.chasoglou@hoganas.com

Abstract—Sinter hardening has been one of the ways to obtain high performance PM low alloyed steel components. The control of the final microstructure and consequently of the mechanical performance of the components is acquired by the suitable process route optimization, namely the cooling rate. The sinter hardening process therefore requires materials with sufficient hardenability which in turn is achieved by chemical composition optimization. This paper presents the properties of a number of materials suitable for sinter hardening processes with regard to mechanical performance as well as material characteristics such as Jominy hardenability tests and CCT diagrams. The materials composition and the respective mechanical properties are correlated by means of metallographic investigation.

Keywords – sinter-hardening, PM steels, Jominy testing, Cr pre-alloyed powders, mechanical properties

I. INTRODUCTION

Over the years a large number of pre-alloyed grades have been released into the market in order for the PM industry to face the challenge of the continuous improvement of the mechanical performance of structural PM parts. Chromium has been an alloying element which has been extensively used in low alloy steel for a long time and has been introduced to PM steels as well since it has great potential in terms of cost, recyclability and health safety as well as performance [1]-[3]. The sensitivity to oxygen by Cr has been one of the main issues connected with the incorporation of Cr via additives which contained large amounts of it (e.g. master alloys, ferrochrome) [4]. This issue was tackled by introducing Cr in the pre-alloyed state which in turn lowers its activity and enables the sintering of the respective materials in conventional mesh belt furnaces at commonly used sintering temperatures (up to 1150°C) provided that a N₂ protective atmosphere containing up to 10% H₂ is used. Of course the

traditional alloying elements such as Ni and Cu are still used in a number of applications and their combination with Cr pre-alloyed materials can lead to a significant boost in performance [5]-[7].

This paper evaluates the mechanical properties of a number of material combinations suitable for sinter hardening. Special focus is put on microstructure optimization by controlling the chemical composition. For this purpose Jominy hardenability testing and quench dilatometry complemented by metallography was also implemented.

II. MATERIALS AND EXPERIMENTAL PROCEDURE

Two Cr pre-alloyed grades (Astaloy CrA and Astaloy CrM) were chosen as base powders for the purposes of this investigation. The nominal composition of these powders is shown in Table 1.

Table 1. Nominal composition of base powders

Base powder	Chemical composition (wt.%)	
	Cr	Mo
Astaloy CrA	1,8	-
Astaloy CrM	3	0,5

Further alloying with different contents of Ni and Cu was also performed in the case of Astaloy CrA by adding elemental powders. All materials were admixed with 0,6% C (UF4), apart from Astaloy CrM which was admixed with 0,5 % C (UF4) and 0,6% Lube E as lubricant. The above are summarized in Table 2.

Table 2. Mixes used in this investigation

Base material	Cu* (wt.%)	Ni* (wt.%)	C (wt.%)	Lube E (wt.%)
Astaloy CrA	-	-	0,6	0,6
Astaloy CrA	2	-	0,6	0,6
Astaloy CrA	-	2	0,6	0,6
Astaloy CrM	-	-	0,5	0,6

*(Admixed)

Tensile, impact and fatigue test specimens according to ISO-standards were compacted using a 60-ton hydraulic compaction press at a standard pressure of 700MPa.

All test specimens were sintered in a mesh belt furnace at 1120°C for 30 minutes in a 90/10 N₂/H₂ atmosphere with carbon potential. The cooling rate for the sinter hardening was approximately 3°C/s.

Tempering at 200°C for 60 minutes in air for stress relief followed the sinter hardening operation.

Plane bending fatigue was tested at R=0 and with a run out limit of 2x10⁶ cycles using the staircase method according to MPIF Standard 56. The endurance limit was determined at 50 % survival.

The CCT diagrams presented in this article were created using the dilatometry curves produced using a Linseis R.I.T.A Quench Dilatometer. Cylindrical samples (Ø: 6mm and height: 10mm) of the materials shown in Table 2 were pressed to a density of 6,8-6,9 g·cm⁻³. In turn the samples were sintered at 1120°C for 30' in a N₂/H₂ – 90/10% atmosphere with carbon potential. The sintered samples were then induction heated (10 °C/s) up to the austenization temperature (960°C) where they were held for 3 minutes and then were cooled down at different cooling rates (from 0,1°C/s up to 200°C/s) using He gas which was also the atmosphere used throughout heating and isothermal holding as well. Metallographic investigation followed for all the samples. The CCT curves were produced using the equipment software WinZTU after the phase transformation points were identified from every dilatometry curve.

For the determination of the hardenability of the chosen materials, the Jominy hardenability test was performed according to ASTM standards [9]. Studies have shown that the Jominy test is suitable for determining the hardenability of PM steels [10]. For performing such Jominy tests, at first the material blends mentioned in Table 2 were pressed into rectangular bars of the following dimensions L:120mm, W:30mm, H:30mm at a density of 7,2 g·cm⁻³. The bars were then sintered at 1120°C for 30' in a N₂/H₂ – 90/10% atmosphere with carbon potential. From the sintered rectangular bars cylindrical samples were machined in the relevant geometry and dimensions (Ø: 25mm in the quench end and

height: 100mm). The produced bars were then heated up to 900°C where they were held for 30' and in turn were inserted to the Jominy test apparatus where the bottom end was subjected to water quenching. The quenched bars were ground in order to avoid the potentially decarburized surface and hardness measurements (Rockwell C) as well as microhardness measurements HV 0,1 were performed along the length of the bar from the quenched end.

III. RESULTS

A. Mechanical Properties

The sample densities and the C-content after sintering are given in Table 3. The apparent hardness and the tensile strength of the sinter hardened specimens are shown in Figures 1 and 2. It is evident that the lower alloying content of the plain Astaloy CrA, is the determining factor for the lower observed value.

Table 3. Densities and C-content after sintering

Material	Sintered Density (g·cm ⁻³)	C-content (wt.%)
Astaloy CrA	7,08	0,53
Astaloy CrA+2Cu	7,06	0,54
Astaloy CrA+2Ni	7,23	0,53
Astaloy CrM	7,1	0,44

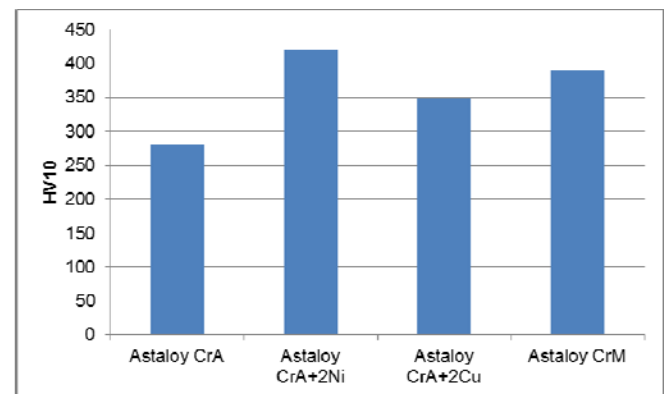


Fig. 1. Apparent hardness (HV10) for sinter hardened Astaloy CrA (with and without Ni and Cu additions) and Astaloy CrM

From the alloying additions to Astaloy CrA, Ni has a stronger effect on apparent hardness compared to Cu, whereas for the tensile strength the same trend is not observed. For the fatigue strength the values that can be reported so far concern only Astaloy CrA with 2% Ni addition and Astaloy CrM (Table 4).

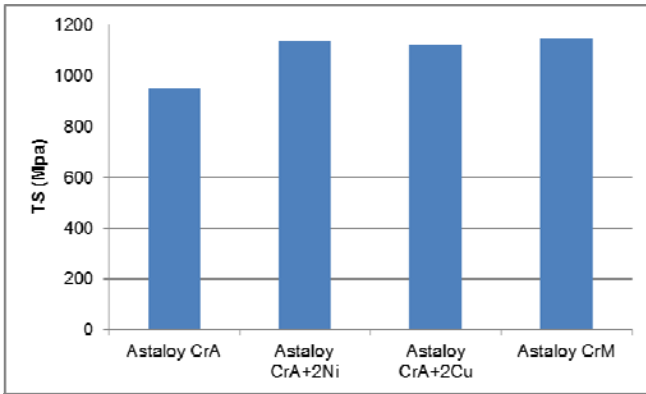


Fig. 2. Tensile strength for sinter hardened Astaloy CrA (with and without Ni and Cu additions) and Astaloy CrM

Table 3. Bending Fatigue strength for selected alloys

Material	Bending fatigue strength (MPa)
Astaloy CrA+2Ni	349
Astaloy CrM	360

Jominy hardenability curves have been obtained for all the alloys under investigation but as an example the one from Astaloy CrA (+0,6C) is shown in Figure 3.

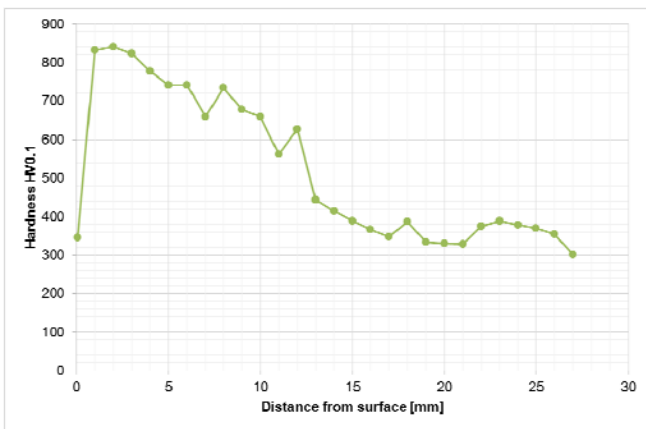


Fig. 3. Jominy hardenability curve for Astaloy CrA

The respective microstructures from the Jominy hardenability test for Astaloy CrA at 1mm, 8,5mm and 20mm from the quench end are shown in Figures 4-6. It is evident that in the surface the martensitic structure is responsible for the high values of HV0,1 observed. With increasing distance from the quench end, the cooling rate has been decreasing and consequently the amount of bainite (the dark phase in Figures 5 and 6) increasing resulting in decrease in microhardness values.

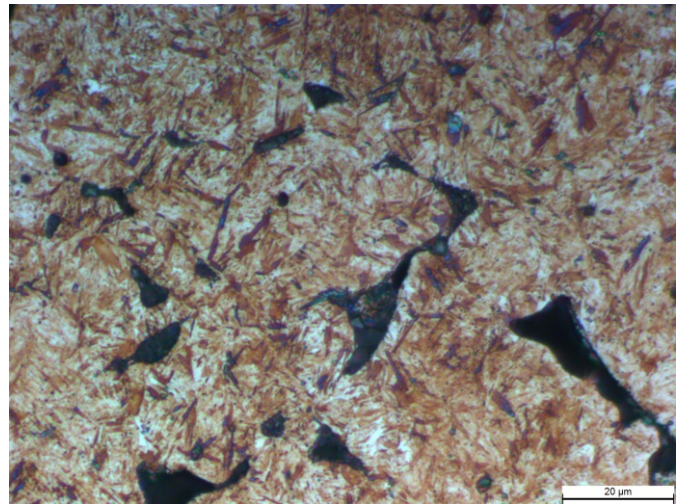


Fig. 4. Microstructure of Astaloy CrA at 1mm from the quench end of the Jominy bar

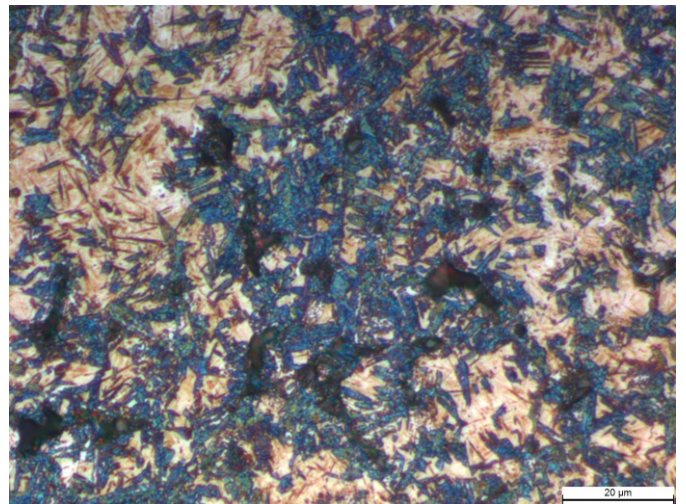


Fig. 5. Microstructure of Astaloy CrA at 8,5mm from the quench end of the Jominy bar

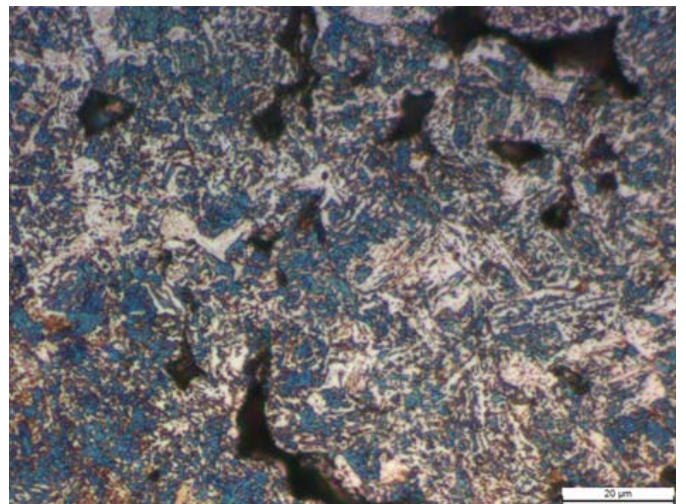


Fig. 6. Microstructure of Astaloy CrA at 20mm from the quench end of the Jominy bar

The effect of Ni on the hardenability is clearly seen on the respective microstructures at the center of the sinter hardened specimens (Figure 7)

where the amount of bainite is significantly reduced. However due to the Ni additions austenitic areas are also observed (white phases). With the above in mind it is expected that a further improvement in all properties would be accomplished with higher sintering temperatures which apart for the pore rounding and densification, also will result in a better distribution of the added Ni and consequently in a more homogenous microstructure.

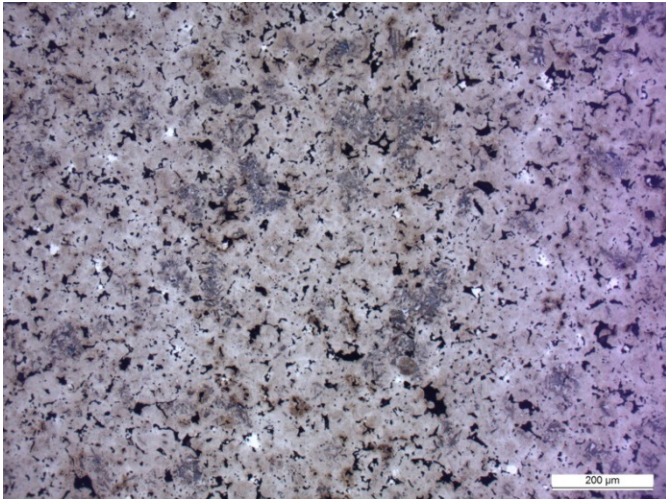


Fig. 7. Microstructure of Astaloy CrA+2Ni at the center of sinter hardened specimens.

All the above can be verified by experimentally derived CCT diagrams as the one shown in Figure 8 for Astaloy CrA containing 0.6%C.

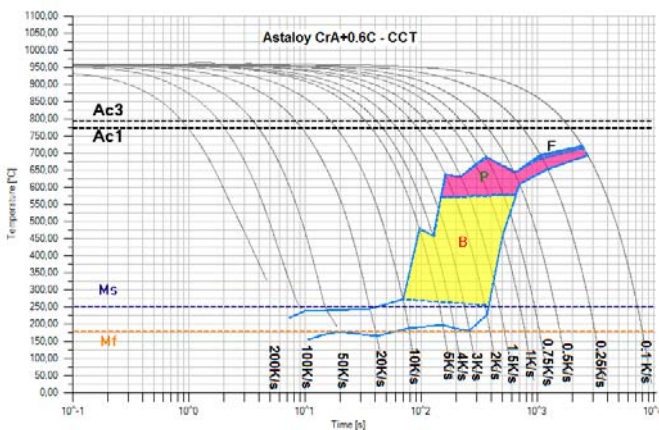


Fig. 8. CCT diagram of Astaloy CrA-0.6C

It is obvious that for the normally applied cooling rates during sinter hardening Astaloy CrA by itself will result in a mixture of martensitic-bainitic microstructure and therefore for higher mechanical performance the additional alloying with Cu or Ni or the higher alloyed Astaloy CrM is recommended.

IV. CONCLUSION

This paper showed the versatility of the Cr pre-alloyed grades that are available today for sinter hardening and which, depending on the intended application, can offer a wide variety of microstructures with the respective mechanical properties.

REFERENCES

- [1] Maroli, S. Berg, P. Thorne, U. Engström, *PM2TEC 2003 International Conference on Powder Metallurgy & Particulate Materials*, Las Vegas, USA, June 10, 2003, vol. 5, pp. 149-161.
- [2] S. Berg, *PM2TEC 2001 World Congress on Powder Metallurgy & Particulate Materials*, New Orleans, USA, May 17, 2001, vol. 5, pp. 18-25.
- [3] O. Bergman, D. Chasoglou, M. Dahlström, *World PM2016 Congress and Exhibition*, Hamburg, Germany, October 9, 2016, Fatigue I.
- [4] D. Chasoglou, E. Hryha, L. Nyborg, *Materials Chemistry and Physics*, 2012, 138 (1), pp. 405-415
- [5] C. Larsson, U. Engström, S. Berg, *Euro PM2012 Congress and Exhibition*, Basel, Switzerland, September 19, 2012, vol. 1, pp. 259-264.
- [6] C. Larsson, U. Engström, *Powder Metallurgy*, 2012, vol. 55, Issue 2, pp. 88-91.
- [7] U. Engström, D. Milligan, A. Klekovkin, *Adv. in Powder Metallurgy & Particulate Materials*, 2006, vol. 1, Part 7, pp. 21-32.
- [8] G. F. Bocchini, B. Rivolta, G. Silva, E. Poggio, M. R. Pinasco, M. G. Ienco, *Powder Metallurgy*, 2004, vol. 47 (4), pp. 343-51.
- [9] Standard Test Methods for Determining Hardenability of Steel A255-02, 2002nd ed. *ASTM International*, 2002.
- [10] G. F. Bocchini, B. Rivolta, A. Baggioli, M. G. Ienco, and M. R. Pinasco, *Powder Metallurgy*, July 2013, vol. 49 (2), pp. 118-124.